Eurographics Workshop on Natural Phenomena (2009)
E. Galin and J. Schneider (Editors)

Corotated SPH for deformable solids

Markus Becker Markus Ihmsen Matthias Teschner

University of Freiburg

Abstract

Smoothed Particle Hydrodynamics (SPH) is a powerful technique for the animation of natural phenomena. While early SPH approaches in Computer Graphics have mainly been concerned with liquids or gases, recent research also focuses on the dynamics of deformable solids using SPH. In this paper, we present a novel corotational SPH formulation for deformable solids. The rigid body modes are extracted from the deformation field which allows to use a linear strain tensor. In contrast to previous rotationally invariant meshless approaches, we show examples using coplanar and collinear particle data sets. The presented approach further allows for a unified meshfree representation of deformable solids and fluids. This enables the animation of sophisticated phenomena, such as phase transitions. The versatility and the efficiency of the presented SPH scheme for deformable solids is illustrated in various experiments.

Categories and Subject Descriptors (according to ACM CCS): Computer Graphics [I.3.7]: Three-Dimensional Graphics and Realism: —Animation

1. Introduction

Meshless (particle-based) approaches are becoming more and more popular in Computer Graphics nowadays, as they bring along several interesting properties. In the computer-based animation of natural phenomena, they can be used for the unified modeling of different material types and their interactions. Uniform object representations and simulation techniques simplify the interface handling among different materials like fluids and solids. They further enable the handling of sophisticated phenomena, such as phase transitions. Several approaches for unified handling based on particles have been proposed in the past [SSP07, MKN*04, BTT09].

Smoothed Particle Hydrodynamics (SPH) is a commonly employed simulation technique. It has been successfully applied to the simulation of a large variety of phenomena such as fire [SF95], deformable solids [DC96], liquids [MCG03, BT07, APKG07, KAD*06], fluid control [TKPR06] and cloth [LAD08].

In the context of SPH, a very promising approach to the uniform handling of different material types has been presented in [SSP07]. Liquids and deformable objects are uniformly represented and processed with SPH. Compared to earlier approaches [Ton91, SoApC*99, CMRBVHT02], Solenthaler et al. [SSP07] have presented a wide range of fluid-solid interaction effects. Effects such as melting and solidification can be handled.

On the other hand, corotational formulations have proven to be a powerful tool for mesh-based deformation models to handle deformable solids at high frame rates. We adopt the corotational concept to the SPH-based deformation model presented in [SSP07]. This enables the use of a linear strain tensor and addresses the erroneous rotation handling in [SSP07].

1.1. Contribution

We propose a novel corotational formulation for meshless deformable solids based on SPH. The proposed approach allows to use a linear strain tensor. We therefore adopt the original corotational idea for the Finite Element Method (FEM) [MDM*02, HS04] to SPH. The rotations in the deformation field are computed using an SPH variant of the shape matching method [MHTG05]. In contrast to meshless approaches based on MLS [MKN*04], we can handle coplanar and collinear particle configurations. Several experiments illustrate the versatility and performance of our technique. We additionally present some results for stable rotation extraction for 1D and 2D objects using Singular Value Decomposition (SVD).

2. Related Work

In Computer Graphics, deformable objects are simulated with a large variety of approaches such as finite difference methods [TPBF87], mass-spring systems (MSS) [BW98, THMG04], implicit surfaces [DC95], the Boundary Element Method (BEM) [JP99], the Finite Element Method (FEM) [DDCB01], the Finite Volume Method (FVM) [TBHF03], and mesh-free particle systems [DC96, Ton98, MKN*04]. For an excellent survey, we refer the reader to [NMK*06].

In our work, we focus on the physically motivated simulation of elasto-mechanical properties using a mesh-free particle system approach, namely SPH. In Computer Graphics, early particle approaches have been presented for softening and melting [TPF89, Ton91] or for viscous fluids [MP89]. In [PTB*03], a particle-based fluid simulator is proposed that employs the moving particle semi-implicit method (MPS). In [CBP05], springs are adaptively incorporated in a particle-based fluid simulation to model visco-elastic fluids. An early SPH approach for the animation of viscous fluids and plastically deformable objects has been proposed by Desbrun and Cani [DC96], while in [PPLT06], melting is modeled with SPH by the transition of high-viscous non-Newtonian fluids to low-viscous fluids. In [AOW*08], a meshless Finite Element method is used for deformable shape modeling. In [WSG05], an approach to model thin shells for point-sampled objects is presented.

A unified particle-based approach to model elastic, plastic and melting behavior of objects has been proposed by Müller et al. [MKN*04]. In this approach, elastic forces are computed using an isotropic, linear stress-strain relation and the non-linear Green-Saint-Venant strain tensor. In order to approximate the Jacobian of the deformation vector field, a Moving Least Squares (MLS) approach is employed. The approach guarantees that an undeformed object is strain-free under rigid body motion. However, for the computation of the Jacobian, an inversion of the moment matrix is required. For coarsely sampled or coplanar particle sets, this moment matrix is singular and cannot be inverted. The approach of [MKN*04] is enhanced in [KAG*05]. In this approach, the Navier Stokes equations are merged with the equations for deformable solids to handle the physical animation of solids, fluids and phase transitions.

In contrast to [MKN*04, KAG*05], Solenthaler et al. [SSP07] use SPH to approximate the Jacobian of the deformation field. Coarsely sampled and coplanar particle configurations can be handled with this approach. However, as the approach cannot distinguish rotation from shear stress, initial orientations of an object are erroneously preserved and thereby rotations are prevented. We extend the approach of [SSP07] by extracting the local orientations of the object from the deformation field and calculating the elastic forces in a rotated configuration. Rotations are therefore not misinterpreted as a deformation of the body and are handled correctly.

The employed idea of a corotational formulation has first been addressed by Capell et al. [CGC*02] to allow for a linear strain tensor. The approach divides an object into small parts. Each part is rotated prior to the computation of the linearly elastic forces. This procedure, however, results in discontinuities at the boundary between adjacent parts. This issue has been addressed in the stiffness warping method by Müller et al. [MDM*02], where individual rotations are computed per vertex, yielding smaller discontinuities. Further improvements have been presented in [MG04, HS04] to avoid ghost forces. We adopt the corotational idea for our meshless simulation by extracting a rotation for each particle based on its neighborhood.

Various methods have been proposed to estimate the relative orientation of two particle sets. An excellent survey can be found in [LEF95]. Since the corresponding particle pairs are a priori known in our approach, we propose an SPH variant of the shape matching method [MHTG05] to compute the optimal rigid transformation between the deformed and the undeformed particle set.

In the context of phase transitions, Losasso et al. [LIGF06] presented an approach for the transition between Lagrangian solids and Eulerian fluids. However, different data structures need to be synchronized to allow for mass transfer. Melting has been addressed in [REN*04] by using high-viscous fluid simulations. In [GBO04], elastic stress has been added to the Navier-Stokes equations to model visco-elastic fluids with an Eulerian fluid solver. Although our approach does not focus on phase transitions, we present experiments that illustrate the utility of the approach in this context.

3. SPH

As we employ SPH, its basic idea is briefly described. In SPH, a function $f(\mathbf{x}_i)$ is approximated as a smoothed function $\langle f(\mathbf{x}_i)\rangle$ using a finite set of sampling points $\mathbf{x}_j$ with mass m_j, density ρ_j, and a kernel function $W(\mathbf{x}_{ij},h) = W(\mathbf{x}_i-\mathbf{x}_j,h)$ with influence radius h. According to Gingold and Monaghan [GM77] and Lucy [Luc77], the original formulation of the smoothed function is

$$\langle f(\mathbf{x}_i)\rangle = \sum_j \frac{m_j}{\rho_j} f(\mathbf{x}_j) W(\mathbf{x}_{ij},h). \qquad (1)$$

Using SPH, derivatives can be calculated by shifting the differential operator to the kernel function [MCG03, BT07]. This can be used to solve the differential equations arising for deformable solids. In the following, we assume that our objects are discretized into a finite set of particles. The neighborhood of a particle i is precomputed. It is defined by the particles j that are located within the influence radius of i, i. e. $W(\mathbf{x}_{ij},h) > 0$, in the initial configuration.

4. Linear elasticity

In this section, we introduce the basic equations for linear elasticity. For a detailed introduction see e. g. [Bat95].

The continuous displacement field of a deformable body is described by $\mathbf{u} = [u, v, w]^T$. For each body position, the displacement corresponds to the difference between the original position $\mathbf{x}^0$ and the current position $\mathbf{x}$. The Jacobian of the mapping $\mathbf{x}^0 \mapsto \mathbf{x}^0 + \mathbf{u}$ is given by $\mathbf{J} = \nabla\mathbf{x}^0 + \nabla\mathbf{u}^T = \mathbf{I} + \nabla\mathbf{u}^T$ with $\mathbf{I}$ denoting the identity matrix. Now, the strain ε is computed using either the non-linear Green-Saint-Venant strain tensor

$$\varepsilon = \frac{1}{2}(\mathbf{J}^T\mathbf{J} - \mathbf{I}) \tag{2}$$

or the linear Cauchy-Green strain tensor

$$\varepsilon = \frac{1}{2}(\mathbf{J} + \mathbf{J}^T) - \mathbf{I} \tag{3}$$

For a linear elastic material, the stress σ linearly depends on the strain ε with $\sigma = \mathbf{C}\varepsilon$. For isotropic materials, the matrix $\mathbf{C} \in \mathbb{R}^{6\times6}$ is characterized by two independent coefficients, namely the Young modulus E and the Poisson ratio ν [Bat95].

Various meshless approaches to calculate elastic forces for a deformed elastic solid have been proposed so far. They basically differ in how to calculate $\nabla\mathbf{u}$ and thereby the Jacobian $\mathbf{J}$. [Hie07] uses a differential update for the deformation gradient which allows to discard the initial particle configuration. A periodic reinitialization is used to maintain consistency. [SSP07] calculates the deformation gradient using an SPH approximation. As discussed later, their formulation is, however, not rotationally invariant due to a low consistency order. [MKN*04, KAG*05] compute the deformation gradient using MLS. As they, however, need to invert a moment matrix for each particle based on its neighborhood, they cannot handle sparse, coplanar and collinear settings.

The presented approach is based on the SPH approximation of [SSP07], but resolves the rotation handling. The original approach is briefly revisited here. In order to compute the elastic force of a particle i, the strain energy U_i is considered as

$$U_i = \tilde{v}_i \frac{1}{2}(\varepsilon_i \sigma_i) \tag{4}$$

with $\tilde{v}_i$ being the initial volume of particle i. The volume $\tilde{v}_i$ does not change and can be precomputed as

$$\tilde{v}_i = \frac{m_i}{\sum_j m_j W(\mathbf{x}^0_{ij}, h)} = \frac{m_i}{\rho_i}. \tag{5}$$

The gradient $\nabla\mathbf{u}_i$ of the displacement field is approximated using SPH as

$$\nabla\mathbf{u}_i = \sum_j \tilde{v}_j \mathbf{u}_{ji} \nabla W(\mathbf{x}^0_{ij}, h)^T. \tag{6}$$

The vector $\mathbf{u}_{ji}$ denotes the differences between the displacement vectors of neighboring particles j and i:

$$\mathbf{u}_{ji} = \mathbf{u}_j - \mathbf{u}_i = \mathbf{x}_j - \mathbf{x}_i - (\mathbf{x}^0_j - \mathbf{x}^0_i). \tag{7}$$

Similar to [MKN*04], we assume that the stress and the strain are constant in the rest volume of each particle. The elastic forces $\mathbf{f}_{ji}$ exerted on particle j by particle i can then be computed as

$$\mathbf{f}_{ji} = -\nabla_{\mathbf{u}_j} U_i = -\tilde{v}_i(\mathbf{I} + \nabla\mathbf{u}_i^T)\sigma_i \mathbf{d}_{ij} \tag{8}$$

with

$$\mathbf{d}_{ij} = \tilde{v}_j \nabla W(\mathbf{x}^0_{ij}, h). \tag{9}$$

for the nonlinear Green-Saint-Venant strain tensor. For the linear Cauchy-Green tensor, (8) simplifies to

$$\mathbf{f}_{ji} = -\tilde{v}_i \sigma_i \mathbf{d}_{ij} \tag{10}$$

As the approximation in (6) is only zero-order consistent (i. e. only constant polynomials are reproduced exactly), it is not rotationally invariant. Instead, rotations are misinterpreted as deformations, resulting in forces that prevent a body from rotating [Sch05]. This is illustrated in Fig. 1 with a simple example.

In their original formulation, both the MLS-based approach and the SPH-based approach use the rotationally invariant non-linear Green-Saint-Venant strain tensor. Motivated by the corotational approaches for FEM, we propose a corotational formulation for the SPH approximation in the next section. This allows to use the linear Cauchy-Green strain tensor, while at the same time handles the rotation problem of the basic SPH algorithm.

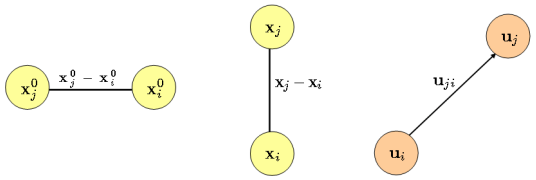

(a) initial configuration (b) after rotation (c) displacement vector

Figure 1: *The erroneous approximation of the gradient $\nabla\mathbf{u}_i$ according to the original SPH approach is illustrated. Therefore, a simple body consisting of two particles i and j is rotated in i. Calculating the deformation gradient from (6) leads to non-zero strain and thereby to non-zero elastic forces.*

5. Corotated SPH for deformable objects

For the mesh-based Finite Element Method, the corotational approach has been successfully applied in the past [MG04, HS04, KMBG08]. It is motivated by the fact that a deformation gradient $\nabla\mathbf{u}$ can always be decomposed into a rotational part and a stretching part. To be able to use the linear

Cauchy-Green strain tensor, which is not rotationally invariant, the rotation is extracted from the deformation gradient and calculated separately.

In this section, we propose a modification of the corotational idea for meshless deformable solids. In our approach, we extract the rotation for each particle directly from the displacement field using a variant of the shape matching approach. The rotation matrix is calculated based on the neighborhood of the particle. This is discussed in Sec. 5.1. The strain and the elastic forces are then calculated on the back-rotated solid, which is discussed in Sec. 5.2. The section is closed with a short discussion in 5.3.

5.1. Calculating the nodal rotations

For our corotational formulation, we want to calculate a rotation $\mathbf{R}_i$ for each particle based on its initial neighborhood. In the shape matching procedure of [MHTG05], the rotation for each object is extracted from the transformation matrix

$$\mathbf{A} = (\sum_i m_i \mathbf{p}_i \mathbf{q}_i^T)(\sum_i m_i \mathbf{q}_i \mathbf{q}_i^T)^{-1} := \mathbf{A}_{pq}\mathbf{A}_{qq}. \tag{11}$$

Here, $\mathbf{q}_i = \mathbf{x}_i^0 - \mathbf{x}_{cm}^0$ and $\mathbf{p}_i = \mathbf{x}_i - \mathbf{x}_{cm}$ are relative particle positions with respect to the center of mass of a body in the initial and the current state, respectively. Since $\mathbf{A}_{qq}$ is symmetric, the orientation $\mathbf{R}$ can be extracted as the rotational part of $\mathbf{A}_{pq}$. This is realized using a polar decomposition $\mathbf{A}_{pq} = \mathbf{RS}$ with the symmetric part $\mathbf{S} = \sqrt{\mathbf{A}_{pq}^T\mathbf{A}_{pq}}$ and the rotational part $\mathbf{R} = \mathbf{A}_{pq}\mathbf{S}^{-1}$. The resulting rotation $\mathbf{R}$ is optimal in the sense of a least square approximation.

Instead of a single rotation matrix $\mathbf{R}$, we compute individual orientations for each particle. Therefore, we propose an SPH formulation for the matrix $\mathbf{A}_{pq}$ for a particle i:

$$\mathbf{A}_{pq_i} = \sum_j m_j W(\mathbf{x}_{ij}^0, h)\left((\mathbf{x}_j - \mathbf{x}_i)(\mathbf{x}_j^0 - \mathbf{x}_i^0)^T\right). \tag{12}$$

The matrix $\mathbf{A}_{pq_i}$ is computed locally considering the initial neighborhood of a particle. The relative distances are weighted by the kernel function to account for the decreasing influence of neighbors with a larger distance, which is similar to [WHP*06]. This is in contrast to [MHTG05], where all points of a cluster equally contribute to the computation. Now, the individual rotation matrix $\mathbf{R}_i$ for a particle i can be computed as

$$\mathbf{R}_i = \mathbf{A}_{pq_i}\mathbf{S}_i^{-1}. \tag{13}$$

In case of a degenerated neighborhood, i. e. a coplanar or collinear setting, we substitute the polar decomposition to calculate $\mathbf{R}_i$ by a stable SVD proposed in [ST08] for the rotation extraction of a deformation gradient. See Sec. 6.4 for some experiments with 1D and 2D objects.

In contrast to our approach, [WHP*06] extracts the rotation from the product of the weighted matrices $\mathbf{A}_{pq}$ and $\mathbf{A}_{qq}$ to estimate initial particle configurations from the deformed state of a meshless deformation approach. As the calculation of the matrix $\mathbf{A}_{qq}$ needs the inversion of a matrix that is similar to the moment matrix in MLS, it is also not suited for coplanar and collinear settings. For 3D examples, both rotation matrices do, however, differ only little in most scenarios.

5.2. Corotated force calculation

Using the rotation matrix calculated in Sec. 5.1, the approximation for the deformation gradient in (6) is now replaced by

$$\nabla \mathbf{u}_i = \sum_j \tilde{\upsilon}_j \bar{\mathbf{u}}_{ji} \nabla W(\mathbf{x}_{ij}^0, h)^T, \tag{14}$$

where $\bar{\mathbf{u}}_{ji}$ is the locally rotated deformation given by

$$\bar{\mathbf{u}}_{ji} = \mathbf{R}_i^{-1}(\mathbf{x}_j - \mathbf{x}_i) - (\mathbf{x}_j^0 - \mathbf{x}_i^0). \tag{15}$$

Finally, the elastic force $\mathbf{f}_i$ at each particle is computed in a symmetrized way as

$$\mathbf{f}_i = \sum_j \frac{-\mathbf{R}_i\bar{\mathbf{f}}_{ji} + \mathbf{R}_j\bar{\mathbf{f}}_{ij}}{2}. \tag{16}$$

$\bar{\mathbf{f}}_{ji}$ and $\bar{\mathbf{f}}_{ij}$ are the forces derived from (8) using the modified deformation gradient in (14).

5.3. Discussion

While the approach of [SSP07] comprises a very versatile model, it is limited in the proper handling of rotations. As the employed deformation gradient is only of zero-order consistency, the rigid body modes do not cancel out, even when using the rotationally invariant Green-Saint-Venant strain tensor. Rotations introduce strain and as a consequence elastic forces into the system. These forces prevent the objects from rotating [Sch05]. Using the rotation handling proposed in the previous sections, this issue is resolved. The modified approach can be applied to the nonlinear as well as the linear strain tensor.

Although we have a lower order of consistency than the MLS-based approach of Mueller et al. [MKN*04], we can stably handle coplanar and even collinear particle data sets.

5.4. Implementation

Similar to [MKN*04], we use spatial hashing [THM*03] to accelerate the search for neighbors and collisions between particles. For the collision detection, we use a non-iterative version of the predictor-corrector scheme presented in [GBF03]. For some scenarios, we geometrically couple a high-resolution surface mesh to the particle data sets.

6. Results

In this section, various experiments are outlined and discussed. We have performed experiments using the linear as well as the non-linear strain tensor. Sec. 6.1 discusses performance issues. Sec. 6.2 illustrates the influence of the simulation parameters and Sec. 6.3 compares the proposed approach with the original SPH approach with respect to rotation handling. Sec. 6.4 illustrates coplanar and collinear settings. Sec. 6.5 shows some complex scenarios and phase transitions. Limitations and directions for further research are discussed in Sec. 7. All experiments have been performed on an Intel Core 2 PC with 2.13 GHz and 2.0 GB of memory.

6.1. Performance

In this section, we compare the presented corotational formulation with two other meshless approaches. We consider a number of cuboids, each consisting of 1000 particles. The particles in each cuboid are arranged on a lattice with a particle distance of 0.1. The influence radius h of the kernel function is 0.2 throughout the measurements. The presented approach is compared to the original SPH approach and a corotational formulation of the original MLS approach of [MKN*04]. Fig. 2 shows the average timings for the calculation of the elastic forces in a single timestep. The linear strain tensor is used in all three approaches. The overall simulation time for a single timestep can be computed by multiplying the force calculation by a constant factor of 2.3 for the original SPH approach, 1.4 for the corotated MLS approach and 1.7 for the corotated SPH approach.

The overhead to the original SPH approach for calculating the rotation matrix results in a factor of 2 for the elastic force computation and of 1.4 for the total simulation step.

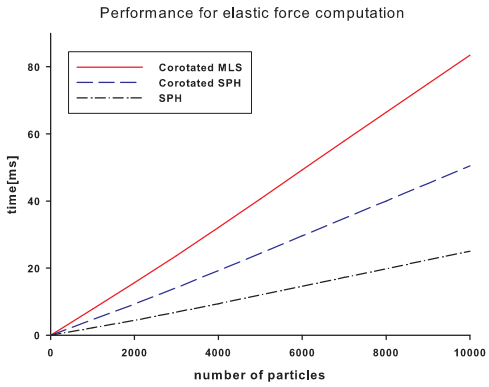

Figure 2: *Performance comparison of [SSP07], a corotated MLS formulation and the proposed corotated SPH approach. The timings are given for the elastic force computations. All three methods scale linearly in the number of particles.*

6.2. Varying material properties

The following two experiments illustrate the capabilities of the corotated SPH approach in the context of deformable solids. Since the nodal rotation matrices are locally computed, the approach can handle a wide range of elasto-mechanical properties. In Fig. 3, two cuboids with identical geometry are attached to a wall. The cuboids consist of 400 particles and have the same mass. The Young moduli are 1000 and 10000. Due to the large deformations, the non-linear strain tensor is used.

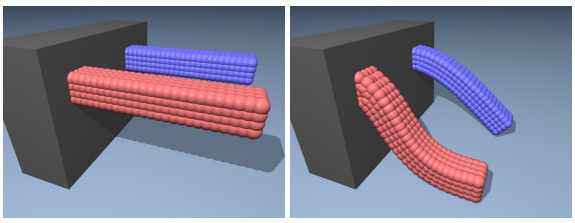

Figure 3: *Two cuboids with Young modulus 1000 and 10000. The left-hand image shows the initial setting, while the right-hand side illustrates the deformations due to gravity.*

As a second example, Fig. 4 illustrates the handling of large deformations such as bending and twisting. Again, the local nature of the nodal orientations enables the wide range of deformations. The non-linear strain tensor is used.

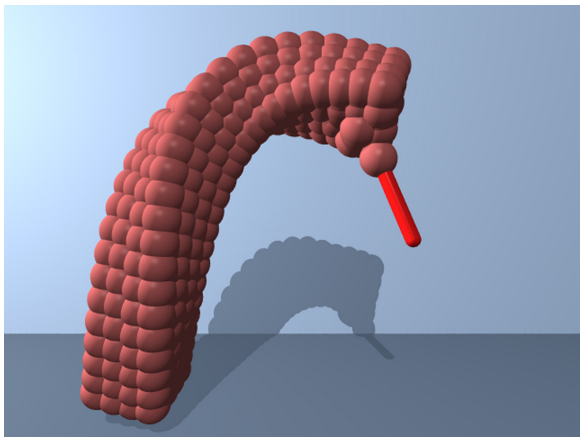

Figure 4: *Large deformations due to user interaction indicated by the red bar. The scenario illustrates that large deformations such as twisting and bending can be simulated with the proposed corotated SPH approach.*

6.3. Rotation handling

In this section, we compare the corotated approach with the original SPH approach with respect to the handling of object rotation. Therefore, we consider a falling cuboid consisting

of 210 particles. For the original SPH approach, we use the non-linear strain tensor. For the corotated approach, we use the linear strain tensor. Using the original SPH approach, the cuboid does not rotate properly throughout the simulation in Fig. 5. In contrast, the cuboid properly rotates if handled by the corotational approach. This is illustrated in Fig. 6.

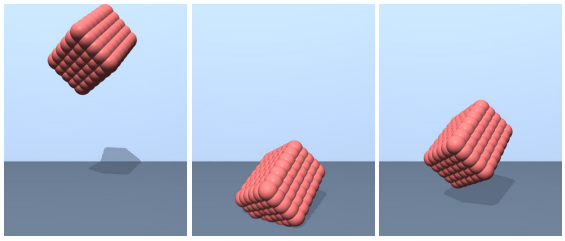

Figure 5: *Sequence of a falling cuboid using [SSP07]. The cuboid deforms, but does not rotate in case of an impact.*

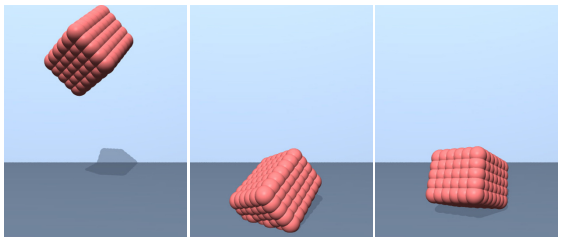

Figure 6: *Sequence of a falling cuboid using the proposed corotational SPH formulation. In contrast to Fig. 5, rotations are properly handled.*

6.4. 1D and 2D objects

To illustrate the proper handling of 2D objects, we simulate a deforming sombrero. The linear strain tensor is used for the calculations. The data set consists of 1800 particles and the average computation time is 25ms. As a second example, we simulate some ducks falling on an elastic membrane. The elastic membrane is represented by a single layer of particles and simulated with a Young modulus E of 15000.

For 1D, we simulate a number of elastic rods falling on two parallel elastic rods. Their stiffness varies from $E = 5 \cdot 10^4$ to $E = 1 \cdot 10^6$. All 1D and 2D examples are illustrated in Fig. 7.

6.5. Complex scenarios

To illustrate the handling of geometrically complex scenarios, Fig. 8 shows the simulation of numerous interacting ducks sliding down a slope. The total number of particles in the scene is 66K. For visualization purposes, a triangulated mesh is geometrically coupled to the particle representations. The average computation time is about 1.5s per simulation step. The proposed approach is also well-suited for

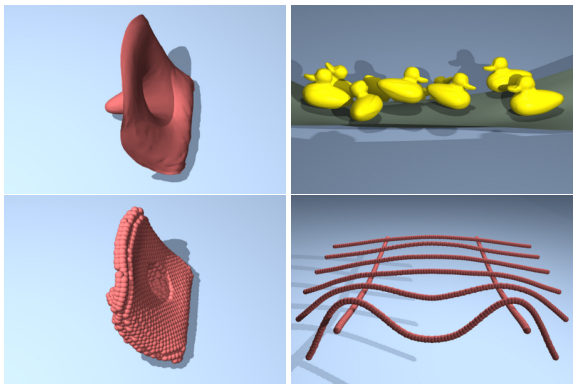

Figure 7: *Upper left and lower left: Surface view and particle view of a deforming elastic sombrero. Top right: Some ducks falling on an elastic membrane. Lower right: A number of elastic rods with varying stiffness falling on two parallel elastic rods.*

phase transitions. Fig. 8 illustrates that we can easily switch between elastic deformation and viscous fluids with our unified model. Surfaces of the fluid are visualized based on a Marching Cubes reconstruction [LC87]. For the fluid simulation, we use the weakly compressible SPH approach proposed in [BT07].

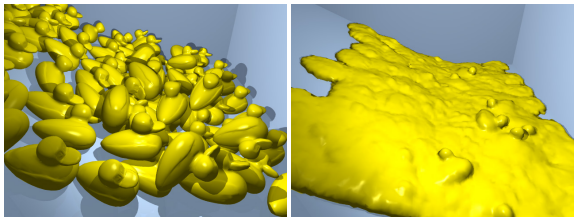

Figure 8: *Interacting deformable ducks sliding down a slope. The ducks melt away on the right hand side.*

Fig. 9 shows a phase transition for a high resolution object. In this example, the cube consists of 100K particles. Both, the elastic surface as well as the fluid surface are reconstructed using Marching Cubes.

7. Conclusion

We have presented a corotational formulation for elastic solids based on SPH. It allows to use the linear Cauchy-Green tensor to calculate elastic forces for a wide range of scenes. For the linear as well as the non-linear strain tensor, it solves the missing rotational invariance of [SSP07]. Our method is capable to simulate large deformations including twisting and bending. The rotation matrices are calculated per particle using a weighted transformation matrix. Our corotational formulation not only improves the realistic behavior of the simulation, but also extends the range of

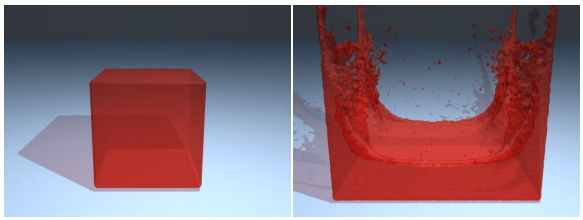

Figure 9: *An elastic cube (left) is transformed into a viscous fluid (right).*

elasto-mechanical properties that can be simulated. In contrast to MLS-based approaches [MKN*04, KAG*05], we perform experiments with coplanar and collinear data sets. Ongoing work focuses on the coupling of elastic solids with particle-based fluid simulations.

References

[AOW*08] ADAMS B., OVSJANIKOV M., WAND M., SEIDEL H.-P., GUIBAS L.: Meshless modeling of deformable shapes and their motion. In *Proc. of Eurographics / ACM SIGGRAPH Symposium on Computer Animation* (2008).

[APKG07] ADAMS B., PAULY M., KEISER R., GUIBAS L. J.: Adaptively sampled particle fluids. In *SIGGRAPH '07: ACM SIGGRAPH 2007 papers* (New York, NY, USA, 2007), ACM Press, p. 48.

[Bat95] BATHE K.: *Finite Element Procedures*, 1st ed. Prentice Hall, 1995.

[BT07] BECKER M., TESCHNER M.: Weakly compressible sph for free surface flows. In *SCA '07: Proceedings of the 2007 ACM SIGGRAPH/Eurographics symposium on Computer animation* (Aire-la-Ville, Switzerland, 2007), Eurographics Association, pp. 209–217.

[BTT09] BECKER M., TESSENDORF H., TESCHNER M.: Direct forcing for lagrangian rigid-fluid coupling. *IEEE Transactions on Visualization and Computer Graphics* (2009). in press.

[BW98] BARAFF D., WITKIN A.: Large steps in cloth simulation. In *Proceedings of SIGGRAPH* (1998), pp. 43–54.

[CBP05] CLAVET S., BEAUDOIN P., POULIN P.: Particle-based viscoelastic fluid simulation. In *SCA '05: Proceedings of the 2005 ACM SIGGRAPH/Eurographics symposium on Computer animation* (New York, NY, USA, 2005), ACM Press, pp. 219–228.

[CGC*02] CAPELL S., GREEN S., CURLESS B., DUCHAMP T., POPOVIĆ Z.: Interactive skeleton-driven dynamic deformations. *ACM Trans. Graph. 21*, 3 (2002), 586–593.

[CMRBVHT02] CARLSON M., MUCHA P. J., R. BROOKS VAN HORN I., TURK G.: Melting and flowing. In *SCA '02: Proceedings of the 2002 ACM SIGGRAPH/Eurographics symposium on Computer animation* (2002), pp. 167–174.

[DC95] DESBRUN M., CANI M.-P.: Animating soft substances with implicit surfaces. In *SIGGRAPH '95: Proceedings of the 22nd annual conference on Computer graphics and interactive techniques* (1995), ACM, pp. 287–290.

[DC96] DESBRUN M., CANI M.-P.: Smoothed particles: A new paradigm for animating highly deformable bodies. In *Eurographics Workshop on Computer Animation and Simulation (EGCAS)* (1996), Springer-Verlag, pp. 61–76. Published under the name Marie-Paule Gascuel.

[DDCB01] DEBUNNE G., DESBRUN M., CANI M.-P., BARR A. H.: Dynamic real-time deformations using space & time adaptive sampling. In *SIGGRAPH '01: Proceedings of the 28th annual conference on Computer graphics and interactive techniques* (2001), ACM, pp. 31–36.

[GBF03] GUENDELMAN E., BRIDSON R., FEDKIW R.: Nonconvex rigid bodies with stacking. *ACM Trans. Graph. 22*, 3 (2003), 871–878.

[GBO04] GOKTEKIN T., BARGTEIL A., O'BRIEN J.: A method for animating viscoelastic fluids. *International Conference on Computer Graphics and Interactive Techniques* (2004), 463–468.

[GM77] GINGOLD R. A., MONAGHAN J.: Smoothed particle hydrodynamics: theory and application to non-spherical stars. *Monthly Notices of the Royal Astronomical Society 181* (1977), 375–398.

[Hie07] HIEBER S.: *Particle-Methods for Flow-Structure Interactions*. PhD thesis, Swiss Federal Institute of Technology, 2007.

[HS04] HAUTH M., STRASSER W.: Corotational simulation of deformable solids. In *In: Proc. WSCG* (2004), pp. 137–145.

[JP99] JAMES D. L., PAI D. K.: Artdefo, accurate real time deformable objects. In *SIGGRAPH '99: Proceedings of the 26th annual conference on Computer graphics and interactive techniques* (1999), ACM Press/Addison-Wesley Publishing Co., pp. 65–72.

[KAD*06] KEISER R., ADAMS B., DUTRÉ P., GUIBAS L., PAULY M.: *Multiresolution Particle-Based Fluids*. Tech. rep., ETH Zurich, 2006.

[KAG*05] KEISER R., ADAMS B., GASSER D., BAZZI P., DUTRE P., GROSS M.: A unified lagrangian approach to solid-fluid animation. In *Proceedings of Eurographics Symposium on Point-Based Graphics* (2005), pp. 125–133.

[KMBG08] KAUFMANN P., MARTIN S., BOTSCH M., GROSS M.: Flexible simulation of deformable models using discontinuous galerkin fem. In *Proc. of the 2008 ACM SIGGRAPH/Eurographics Symposium on Computer Animation* (2008), pp. 105–115.

[LAD08] LENAERTS T., ADAMS B., DUTRÉ P.: Porous flow in particle-based fluid simulations. In *SIGGRAPH '08: ACM SIGGRAPH 2008 papers* (New York, NY, USA, 2008), ACM, pp. 1–8.

[LC87] LORENSEN W. E., CLINE H. E.: Marching cubes: A high resolution 3d surface construction algorithm. In *SIGGRAPH '87: Proceedings of the 14th annual conference on Computer graphics and interactive techniques* (New York, NY, USA, 1987), ACM Press, pp. 163–169.

[LEF95] LORUSSO A., EGGERT D., FISHER R.: A comparison of four algorithms for estimating 3-d rigid transformations. In *Proceedings of the 4th British Machine Vision Conference (BMVC '95)* (1995), pp. 237 – 246.

[LIGF06] LOSASSO F., IRVING G., GUENDELMAN E., FEDKIW R.: Melting and burning solids into liquids and gases. *IEEE Transactions on Visualization and Computer Graphics 12* (2006), 342–352.

[Luc77] LUCY L. B.: A numerical approach to the testing of the fission hypothesis. *The Astronomical Journal 82* (1977), 1013–1024.

[MCG03] MÜLLER M., CHARYPAR D., GROSS M.: Particle-based fluid simulation for interactive applications. In *SCA '03:*

Proceedings of the 2003 ACM SIGGRAPH/Eurographics symposium on Computer animation (Aire-la-Ville, Switzerland, 2003), Eurographics Association, pp. 154–159.

[MDM*02] MÜLLER M., DORSEY J., MCMILLAN L., JAGNOW R., CUTLER B.: Stable real-time deformations. In *SCA '02: Proceedings of the 2002 ACM SIGGRAPH/Eurographics symposium on Computer animation* (New York, NY, USA, 2002), ACM, pp. 49–54.

[MG04] MÜLLER M., GROSS M.: Interactive virtual materials. In *GI '04: Proceedings of Graphics Interface 2004* (School of Computer Science, University of Waterloo, Waterloo, Ontario, Canada, 2004), Canadian Human-Computer Communications Society, pp. 239–246.

[MHTG05] MÜLLER M., HEIDELBERGER B., TESCHNER M., GROSS M.: Meshless deformations based on shape matching. *ACM Trans. Graph. 24*, 3 (2005), 471–478.

[MKN*04] MÜLLER M., KEISER R., NEALEN A., PAULY M., GROSS M., ALEXA M.: Point based animation of elastic, plastic and melting objects. In *SCA '04: Proceedings of the 2004 ACM SIGGRAPH/Eurographics symposium on Computer animation* (2004), Eurographics Association, pp. 141–151.

[MP89] MILLER G., PEARCE A.: Globular dynamics: A connected particle system for animating viscous fluids. *Computers & Graphics 13*, 3 (1989), 305–309.

[NMK*06] NEALEN A., MULLER M., KEISER R., BOXERMAN E., CARLSON M.: Physically Based Deformable Models in Computer Graphics. *Computer Graphics Forum 25*, 4 (2006), 809–836.

[PPLT06] PAIVA A., PETRONETTO F., LEWINER T., TAVARES G.: Particle-based non-newtonian fluid animation for melting objects. *XIX Brazilian Symposium on Computer Graphics and Image Processing (SIBGRAPI'06) 0* (2006), 78–85.

[PTB*03] PREMOZE S., TASDIZEN T., BIGLER J., LEFOHN A., WHITAKER R.: Particle-based simulation of fluids. *Computer Graphics Forum (Proc. of Eurographics) 22* (2003), 401–410.

[REN*04] RASMUSSEN N., ENRIGHT D., NGUYEN D., MARINO S., SUMNER N., GEIGER W., HOON S., FEDKIW R.: Directable photorealistic liquids. In *SCA '04: Proceedings of the 2004 ACM SIGGRAPH/Eurographics symposium on Computer animation* (Aire-la-Ville, Switzerland, Switzerland, 2004), Eurographics Association, pp. 193–202.

[Sch05] SCHLÄFLI J.: *Simulation of Fluid-Solid Interaction*. Master's thesis, University of Zürich, 2005.

[SF95] STAM J., FIUME E.: Depicting fire and other gaseous phenomena using diffusion processes. In *SIGGRAPH '95: Proceedings of the 22nd annual conference on Computer graphics and interactive techniques* (New York, NY, USA, 1995), ACM, pp. 129–136.

[SoApC*99] STORA D., OLIVIER AGLIATI P., PAULE CANI M., NEYRET F., DOMINIQUE GASCUEL J.: Animating lava flows. In *in Graphics Interface* (1999), pp. 203–210.

[SSP07] SOLENTHALER B., SCHLÄFLI J., PAJAROLA R.: A unified particle model for fluid-solid interactions. *Computer Animation and Virtual Worlds 18*, 1 (2007), 69–82.

[ST08] SCHMEDDING R., TESCHNER M.: Inversion handling for stable deformable modeling. *The Visual Computer 24*, 7 (2008), 625–633.

[TBHF03] TERAN J., BLEMKER S., HING V. N. T., FEDKIW R.: Finite volume methods for the simulation of skeletal muscle. In *SCA '03: Proceedings of the 2003 ACM SIGGRAPH/Eurographics symposium on Computer animation* (2003), Eurographics Association, pp. 68–74.

[THM*03] TESCHNER M., HEIDELBERGER B., MUELLER M., POMERANETS D., GROSS M.: Optimized spatial hashing for collision detection of deformable objects. In *Proceedings of Vision, Modeling, Visualization VMVŠ03* (2003), pp. 47–54.

[THMG04] TESCHNER M., HEIDELBERGER B., MÜLLER M., GROSS M.: A versatile and robust model for geometrically complex deformable solids. In *Proc. Computer Graphics International CGI'04* (2004), pp. 312–319.

[TKPR06] THÜREY N., KEISER R., PAULY M., RÜDE U.: Detail-preserving fluid control. In *SCA '06: Proceedings of the 2006 ACM SIGGRAPH/Eurographics symposium on Computer animation* (Aire-la-Ville, Switzerland, Switzerland, 2006), Eurographics Association, pp. 7–13.

[Ton91] TONNESEN D.: Modeling liquids and solids using thermal particles. *Proceedings of Graphics Interface* (1991), 255–262.

[Ton98] TONNESEN D. L.: *Dynamically coupled particle systems for geometric modeling, reconstruction, and animation*. PhD thesis, University of Toronto, 1998.

[TPBF87] TERZOPOULOS D., PLATT J., BARR A., FLEISCHER K.: Elastically deformable models. In *SIGGRAPH '87: Proceedings of the 14th annual conference on Computer graphics and interactive techniques* (New York, NY, USA, 1987), ACM, pp. 205–214.

[TPF89] TERZOPOULOS D., PLATT J., FLEISCHER K.: Heating and melting deformable models. *Graphics Interface* (1989), 219–226.

[WHP*06] WICKE M., HATT P., PAULY M., MÜLLER M., GROSS M.: Versatile virtual materials using implicit connectivity. In *Proceedings of the Eurographics Symposium on Point-Based Graphics* (2006), pp. 137–144.

[WSG05] WICKE M., STEINEMANN D., GROSS M.: Efficient Animation of Point-Sampled Thin Shells. *Computer Graphics Forum 24*, 3 (2005), 667–676.